UNIVERSITY OF OKLAHOMA

GRADUATE COLLEGE

NON-DESTRUCTIVE INDEX TESTING FOR RELATIVE ASSESSMENT OF ROCK STRENGTH

A THESIS

SUBMITTED TO THE GRADUATE FACULTY

in partial fulfillment of the requirements for the

Degree of

MASTER OF SCIENCE

By

ALEX MATHEW VACHAPARAMPIL
Norman, Oklahoma
2016

NON-DESTRUCTIVE INDEX TESTING FOR RELATIVE ASSESSMENT OF ROCK STRENGTH

A THESIS APPROVED FOR THE
MEWBOURNE SCHOOL OF PETROLEUM AND GEOLOGICAL ENGINEERING

BY

_____
Dr. Ahmad Ghassemi, Chair

_____
Dr. Maysam Pournik

_____
Dr. Ahmad Jamili

To you, dearest Susmitha

Who opened my eyes to all that is valuable.

Acknowledgements

I would like to extend immeasurable appreciation and my deepest gratitude towards the following persons for their invaluable help and support that made this study possible:

Dr. Ahmad Ghassemi: my research advisor and committee chair, for his continuous guidance and support, for constantly sharing his insights and ideas, for always sending me the most invaluable research articles, and for the daily lab meetings that constantly shaped the course of this work.

Dr. Ahmad Jamili & Dr. Maysam Pournik: my committee members, for their critical thoughts, discussions and inputs that allowed me to approach research more holistically and through various optics.

Steve Dwyer: our laboratory technologist, for his pragmatic approach and in-depth knowledge of research equipment.

Dr.Xuejun Zhou: for introducing me to research methodology, and for involving me in various projects that deeply enriched my research experience.

Yawei Li: For sharing his vast experience with experimental research.

And to all my other lab mates, it has been an honor to work with you.

Table of Contents

List of Tables

List of Figures

Abstract

Index tests for the determination of rock properties have been employed since the early 90s, based on methods developed since the 1900s in the metallurgical industry. Examples include the Brinell hardness test, Rockwell hardness test, and the Vickers Hardness test. The use of the Brinell hardness tests gained momentum in the domain of rock mechanics in more recent times in response to increased interest in unconventional petroleum and geothermal resource development. Empirical relationships between various rock properties (UCS, Young's Modulus etc.) and index tests data have been established, which are frequently used for rapid determination of reservoir rock properties from index tests. The Brinell hardness test has been the most popular of these, perhaps due to its historical prominence in the metallurgical industry since the 1940s. However, the use of the Brinell hardness test for rock is known to have some major drawbacks, it may become "accidentally destructive" if the rock is too soft, or too hard. Moreover, the test has not been standardized for use in rock mechanics, and various different techniques have been used to perform it, resulting in difficulty in comparing readings from different sources. In this study, we carry out Brinell and rebound hardness experiments on a variety of rock types. Both sets of experimental data show a strong dependence on rock textural characteristics. Furthermore, the data demonstrate a strong correlation between the two index test results. Thus, the rebound hardness tests may be used as a direct substitute for the Brinell hardness test, as it is easier to perform, with reduced chances of specimen destruction, and less sensitive to creep effects. In addition, these index experiments have been performed over a variety of rock types to demonstrate its feasibility.

Chapter 1: Introduction

The first widely recognized index test was proposed by J.A Brinell in the early 1900s. The Brinell hardness method as an indentation test was first used in the iron and steel industry as a method to consistently and rapidly measure the hardness of metals. The technique is still widely used today, and consists of indenting the metal surface with a 1 to 10 millimeter diameter hardened steel (or a tungsten carbide ball) ball at indentation loads of up to 3,000 kgF. The resulting impression (the diameter of the indent) is measured subsequent to removal of the load. An average of two or more readings of the diameter of the impression is made which are then used in mathematical expressions (Equation 1) to obtain a hardness value. Once relationships between Brinell hardness and the yield stress of steel were understood and documented, it came to constitute a means to rapidly perform quality control in the steel production industry.

Later, similar tests (such as the Rockwell, and Vickers Hardness) were developed on similar principles, for specific application on various material types - the differences between these being minor changes to sequence of operations or the shape of the indenter tip being used.

The use of indentation tests in Rock mechanics gained interest in the early 1970's, when correlations between Brinell hardness test results and rock mechanical properties were observed [1-6]. The uniaxial compressive strength as well as the modulus of elasticity have been observed to correlate directly with rock hardness. Specialized equipment to

perform the test across reservoir rock core was subsequently developed [7, 8] and many core logging equipment and techniques today constitutes performing the Brinell hardness test across reservoir rock core at specified intervals.

Scientific progress in the use of index testing later popularized other techniques such as the rebound hammer; and recently, similar correlations between the rebound hammer index and Young's modulus and the unconfined compressive strength have also been found, and rebound hardness has successfully been used as a technique for logging reservoir rock core [9-15]. However, many parts of the petroleum industry continue to use the Brinell hardness test for purposes of rock strength indexing for various reasons despite its various drawbacks and limitations. In this study, we explore various aspects of the Brinell hardness and the rebound hardness techniques, and demonstrate how various problems intrinsic to the former are remedied in the latter method. We then proceed to develop a correlation between the two tests by conducting experiments over a variety of rock types. The correlation may be potentially used as a basis to compare or translate readings across the two tests types.

Chapter 2: Experimental Set-Up and Test Procedure

2.1 Brinell Hardness Testing

In this work a 3 mm diameter chrome coated steel ball is used as the indenter tip (see Figure 1), preliminary investigation with a variety of ball sizes revealed that the use of larger ball sizes induced tensile fracturing in the specimen (loads required to produce measurable impressions were higher than the load required to induce fracturing. The chrome coating minimized surface wear on the balls from repeated indentation, and also provides for a smooth low friction contact between the indenter ball and the rock surface (a low friction contact is necessary to avoid producing artificially large impressions due to frictional effects [16]. For the purpose of indentation testing, various rocks of interest are cored with a 1-inch coring bit to obtain a standard plug. The plugs are then cut with a diamond-wafering blade to obtain disc-shaped rock specimens of 1-inch diameter and 0.4-inch thickness for indentation testing. Cutting the specimens on a precision saw with a diamond wafering blade ensured that the surface smoothness was greater than a 2000 grit surface finish. The flatness of the surface was maintained to within 0.1 mm, by measuring the thickness of the disk at various points along the circumference using a micrometer, this ensured that the indentation surface was leveled horizontally.

We designed and fabricated stainless steel fixtures within which the steel ball could be seated. The fixture features a 1.1-inch diameter recess with a 1 mm diameter hole

drilled at the base, which serves the function of a ball seat (Figure 1). Figure 2 shows a picture of a Berea Sandstone specimen placed into the indentation fixture. To perform an indentation test, the specimen is inserted into the fixture (Figure 2 & 3) and placed on the MTS 810 load frame (Figure 4). Any mechanical press is sufficient for performing indentation tests provided the loads and displacements can be measured using a data acquisition system, and that indentation can be performed under a chosen load.

Figure 1. Indentation Fixture

Figure 2. Berea Sandstone Specimen in Indentation Fixture

A schematic of the test specimen in the indentation fixture is shown in Figure 3. The indentation load is measured through a load cell located on the crosshead of the load frame, and displacements could be measured through the position of the actuator system located at the base of the press (Figure 4).

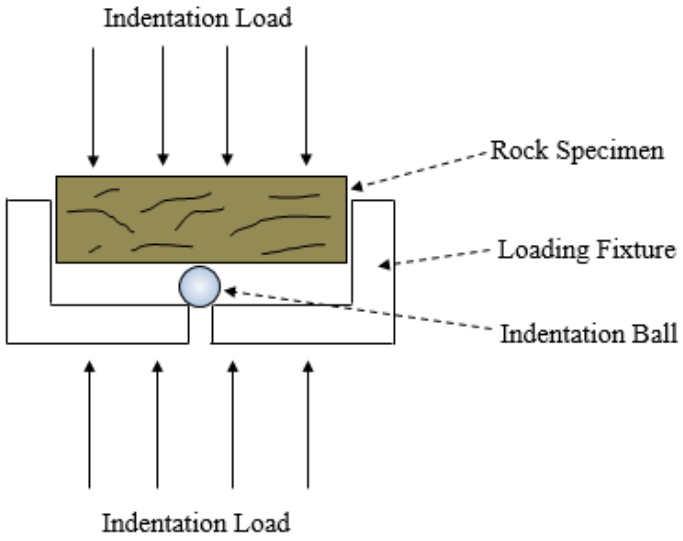

Figure 3.Cross Section Schematic of Loading Fixture

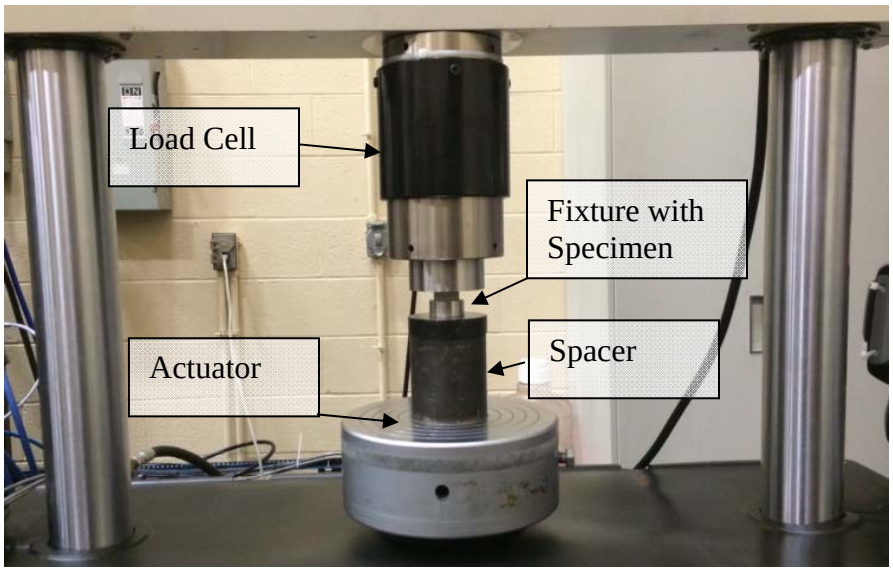

Figure 4.Indentation Fixture in MTS 810 Triaxial Press

The test is performed by indenting a flat rock specimen with a 3 mm indenter ball under a constant load of 0.25 kN (25.5 KgF). The load is held for a time of 30 seconds (the 30 second wait time is given so as to allow the entire process to reach equilibrium) followed by unloading, and measurement of the residual impression using a digital caliper. An average reading from two tests is used to establish the final Brinell hardness using the formula:

$$\mathbf{BHN} = \frac{2P}{\pi a * \left(a - \sqrt{a^2 - d^2}\right)} \quad (1)$$

Where a is the diameter of the ball used and d is the diameter of the impression created on the surface (in mm). Figure 5 shows the measurement of the impression created on a Pierre Shale specimen by the Brinell hardness test. It was found that the size of the impression created by the test had a high degree of repeatability, with the two consecutive impressions differing by less than 0.02 mm.

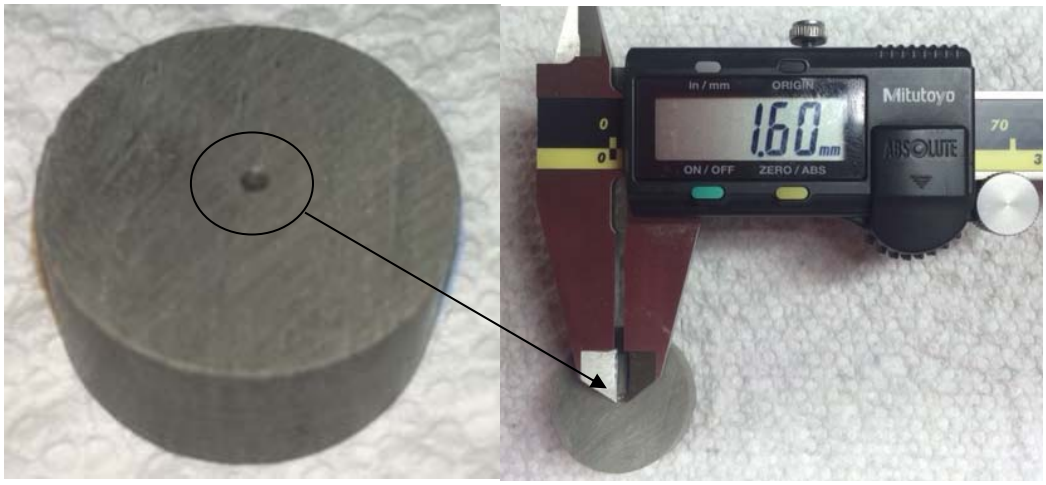

Figure 5.Measurement of Impression on Pierre Shale

One major drawback of Brinell Hardness testing is that it does not lend itself to use on harder rock types such as granite (no measurable impression could be created without inducing fracture propagation), and so igneous and metamorphic rocks cannot be tested. Relatively high loads are needed to create measurable impressions on harder rock types, whereas lower loads are required for softer rocks in order to prevent fracture propagation. As a result, a wide variety of loads cannot be used in the tests across rock types- thereby limiting the scale of investigation.

2.2 Rebound Hardness Testing

Though termed a hardness measurement, rebound hardness is actually a measure of the coefficient of restitution of the rock surface (on a scale of a thousand). A handheld rebound hammer as shown in Figure 5 (also known as the Schmidt Hammer or Bambino Hammer) is used to fire a small steel ball at the rock surface with a known

velocity. The velocity with which the ball bounces back is measured by the device. The coefficient of restitution is then calculated by the instrument using:

$$\textbf{Rebound Hardness} = \mathbf{R} = \frac{\textbf{Rebound Velocity}}{\textbf{Impinging Velocity}} * \mathbf{1000} \quad (2)$$

The coefficient of restitution is a function of the ratio of rebound and impinging kinetic energies of the rebound ball as shown below:

$$\boldsymbol{R} = \frac{\mathbf{V_{Rebound}}}{\mathbf{V_{Impinge}}} = \sqrt{\frac{\left(\frac{\mathbf{mv^2}}{\mathbf{2}}\right)_{\mathbf{Rebound}}}{\left(\frac{\mathbf{mv^2}}{\mathbf{2}}\right)_{\mathbf{Impinge}}}} = \sqrt{\frac{(\mathbf{K.E})_{\mathbf{Rebound}}}{(\mathbf{K.E})_{\mathbf{Impinge}}}} \quad (3)$$

Where m is the mass of the rebound ball, and v is its velocity.

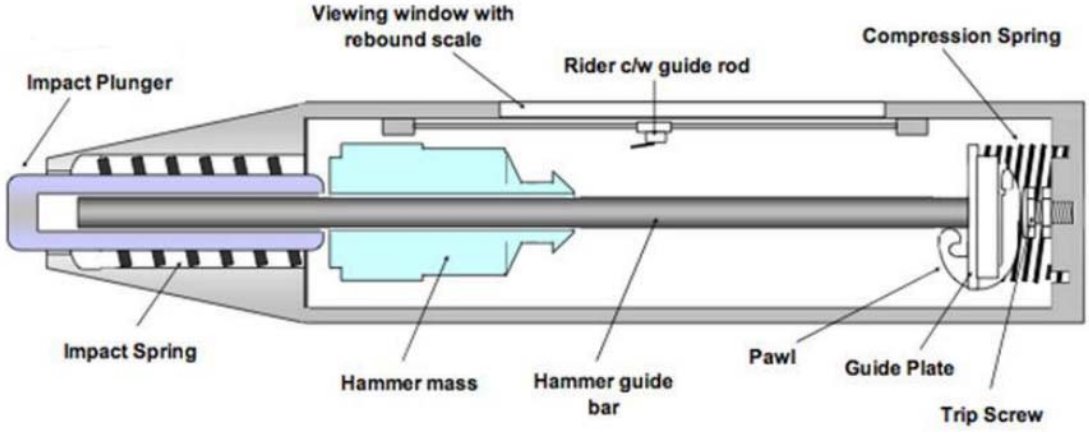

Figure 6. Schematic Cross Section of a Schmidt Rebound Hammer [16]

Figure 6 shows a schematic of the classical Schmidt rebound hammer. It consists of a spring mass system, whereby energy stored in the cocked spring is used to fire the plunger-hammer mass assembly at the test surface. The rebound energy from the test

surface is then used to return the spring to its former position. The energy loss from the collision of the plunger with the test surface is then measured using the extent of the spring return, as read on the rebound dial/scale. The ease with which hammer tests are conducted lends itself to rapid and inexpensive testing over a variety of materials and rock types.

In this work, Hammer tests are performed using the Proceq - Equotip Bambino 2 rebound hammer (essentially a more compact version of the Schmidt hammer, with an electronic scale), on the same disc shaped rock specimens that are later used for Brinell hardness testing. Standard procedure [18] for using the Schmidt hammer calls for a specimen size of $15cm^3$, this minimizes the influence of the working surface. Since large specimens of this size were not available, the samples were seated firmly on a 3 inch thick granite counter top (to minimize any influence of the working surface on the rebound readings), and the hammer was fired onto the specimen surface to obtain a reading (Figure 7).

Ten readings are taken on each rock type to obtain an average value. Readings are taken in the central region of the disk and not near the edges (ASTM D5873 [18] requires that the test location be a distance of at least one rebound ball diameter away from the edges of the specimen).

Figure 7. Rebound Reading on Berea Sandstone

Chapter 3: Results and Inferences

A total of twelve different rock types were tested, composed of four different limestones, four sandstones and four shales. Table 1 lists each tested rock type and the source from which they were procured.

Table 1. Sources for Rock Types Tested

Rock Type		Source
Limestone	Oolitic Limestone	Kocurek Industries
	Indiana Limestone	Kocurek Industries
	Desert Pink Limestone	Kocurek Industries
	Kasota Dolomite	Coldspring Stone Company
Sandstone	Berea Sandstone	Kocurek Industries
	Scioto Sandstone	Kocurek Industries
	DunnVille Sandstone	Coldspring Stone Company
	JackFork Channel Sandstone	Baumgartner Quarry, Arkansas
Shale	Mancos Shale	Kocurek Industries
	Pierre Shale	Kocurek Industries
	Barnett Shale	Kocurek Industries
	Green River Shale	Parachute Quarry, Colorado

The mineralogy for each of the above rock type was assessed via x-ray diffraction (XRD); the mineralogy reports have been presented in Appendix A.

Table 2 shows the Brinell and rebound hardness values obtained for various rocks; this is graphically represented in Figure 8. The Young's Modulus for some of these rock types has also been provided as a reference (from uniaxial tests)[19].

Table 2. Table of Hardness Results Across Rock Types.

	Rock	BHN	Rebound Hardness	Young's Modulus
		KgF/mm^2	-	(GPa)
Carbonate	Oolitic Limestone	18.41	401.2	13.2
	Indiana Limestone	36.23	419.1	18.67
	Desert Pink Limestone	13.89	325	5.35
	Kasota Dolomite	90.95	514.4	-
Siliceous	Berea Sandstone	49.22	510	22.58
	Scioto Sandstone	104.49	536.1	17.68
	DunnVille Sandstone	22.79	435.2	-
	JackFork Channel Sandstone	87.93	538.1	17.96
Shale	Mancos Shale	131.93	596.6	20.76
	Pierre Shale	12.30	324.3	2.48
	Barnett Shale	25.00	449.3	10.08
	Green River Shale	202.34	656.7	-

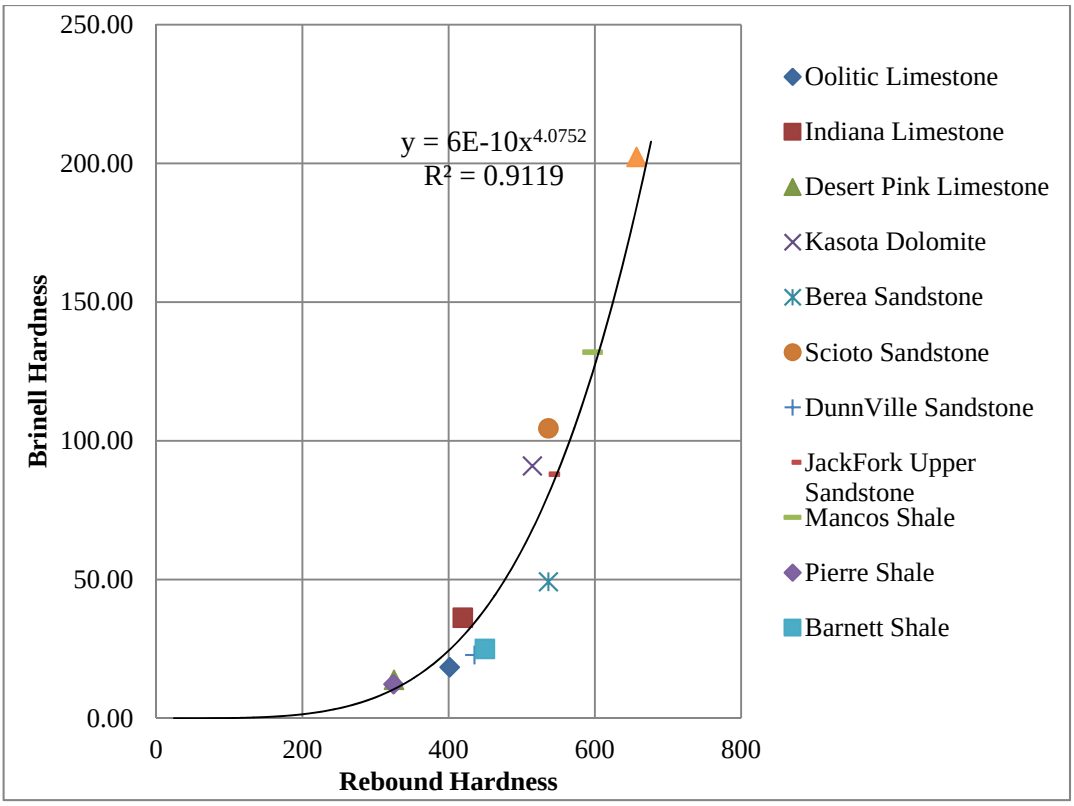

Figure 8. Brinell Hardness vs. Rebound Hardness.

As can be seen, there is a strong relationship between the Brinell and rebound hardness indices across various rock types. The following correlation may then be used to compare or translate readings taken from either test type.

$$\mathrm{BHN} = 6\mathrm{x}10^{-10}(\mathrm{RH})^{4.075} \qquad (4)$$

Where "BHN" is the Brinell hardness and "RH" is the Rebound hardness. Although the repeatability of Brinell hardness was higher than that of the rebound hardness (Brinell Hardness has a mean standard deviation of 4.43, whereas the rebound hardness has a mean standard deviation of 31.72 – see Appendix B), it was observed that some rocks (particularly the softer types) displayed different Brinell hardness numbers depending

upon the duration for which the indentation loads were held before unloading. Longer load stages yielded lower hardness numbers due to enlargement of the surface cavity by material creep. Figure 9 shows a plot of depth of penetration vs. time for Pierre shale in the Brinell hardness test.

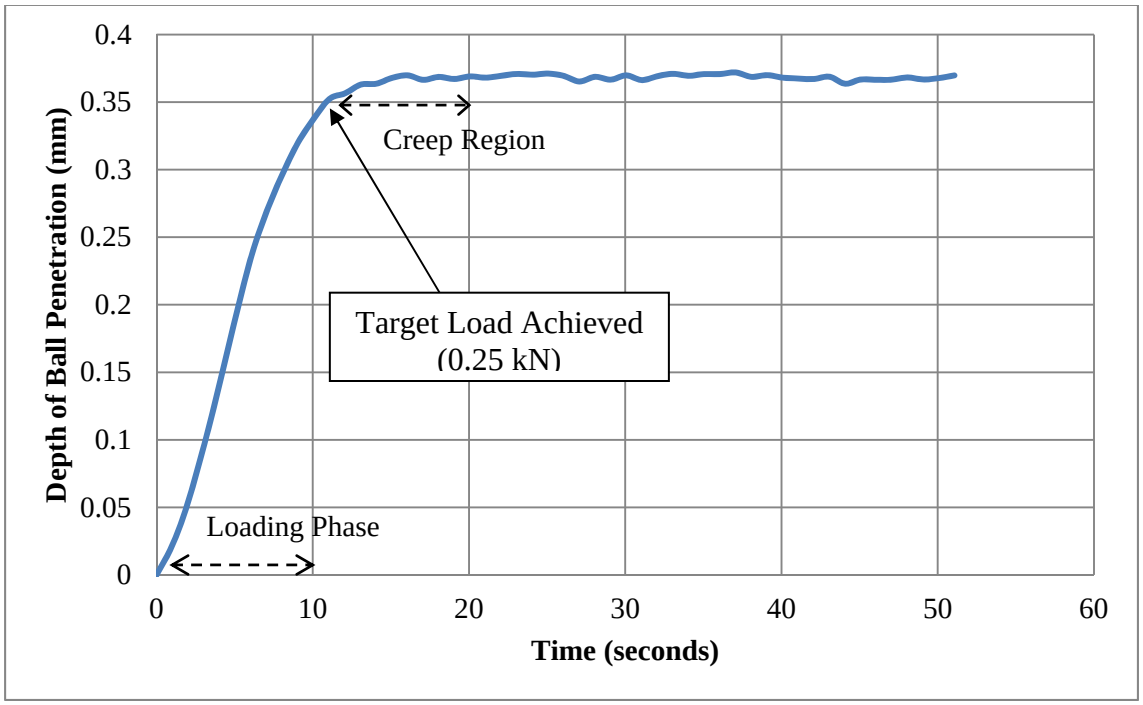

Figure 9. Indentation Creep in Pierre Shale

Note that deformation continues for a short time even after completion of the loading phase. While this is partially remedied by using a common time interval of 30 seconds for the test across all rock types, it remains a source uncertainty and is one potential cause for the data scatter observed in Figure 8.

Chapter 4: Effects of Rock Texture On Index Values

Thin sections were taken for two rock types from each of the three groups (limestone, sandstone, shale) and have been presented below along with some observations about their textural properties. Blue epoxy stain was used to differentiate the pore spaces, and alizarin stain was used to color calcite in pink.

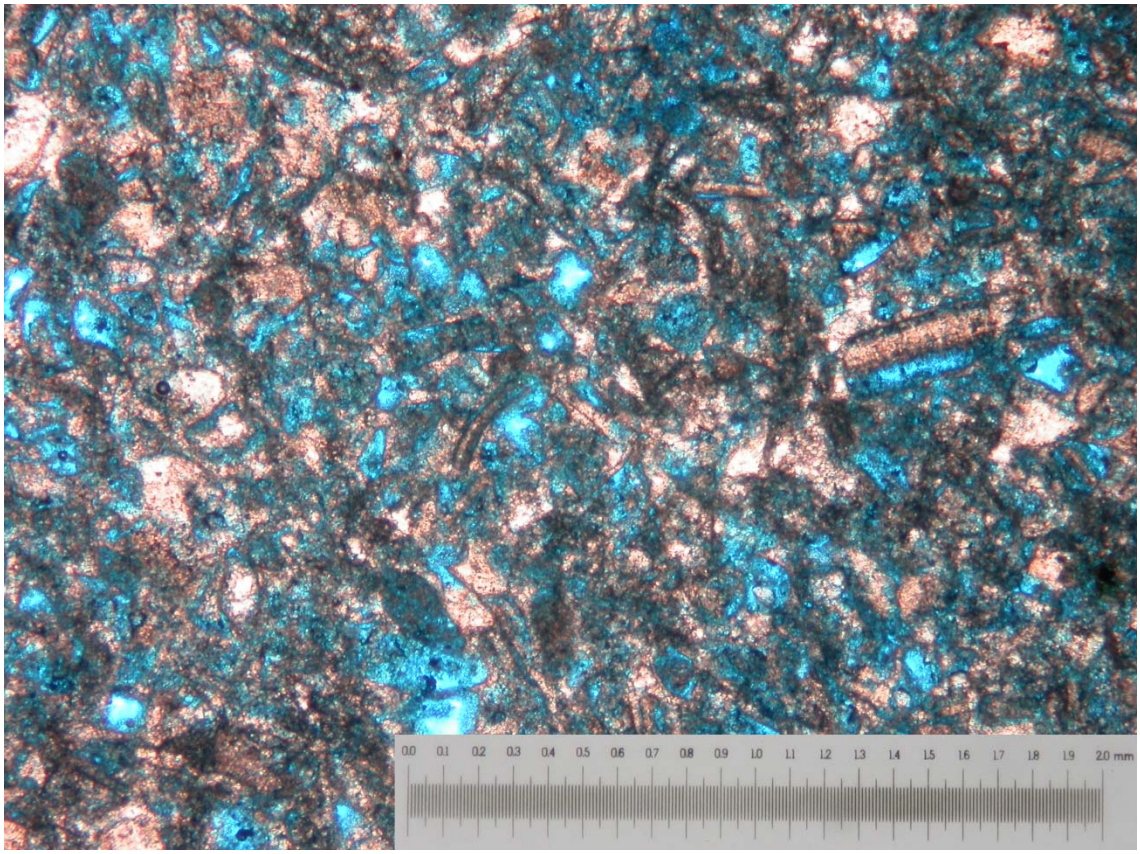

Figure 10. Thin Section – Desert Pink Limestone

Overall, Desert Pink Limestone is composed of marly calcareous fragments. The porosity of this rock is very high as evidenced by the large amount of area occupied by the blue epoxy filler. Pores are mostly moldic in nature.

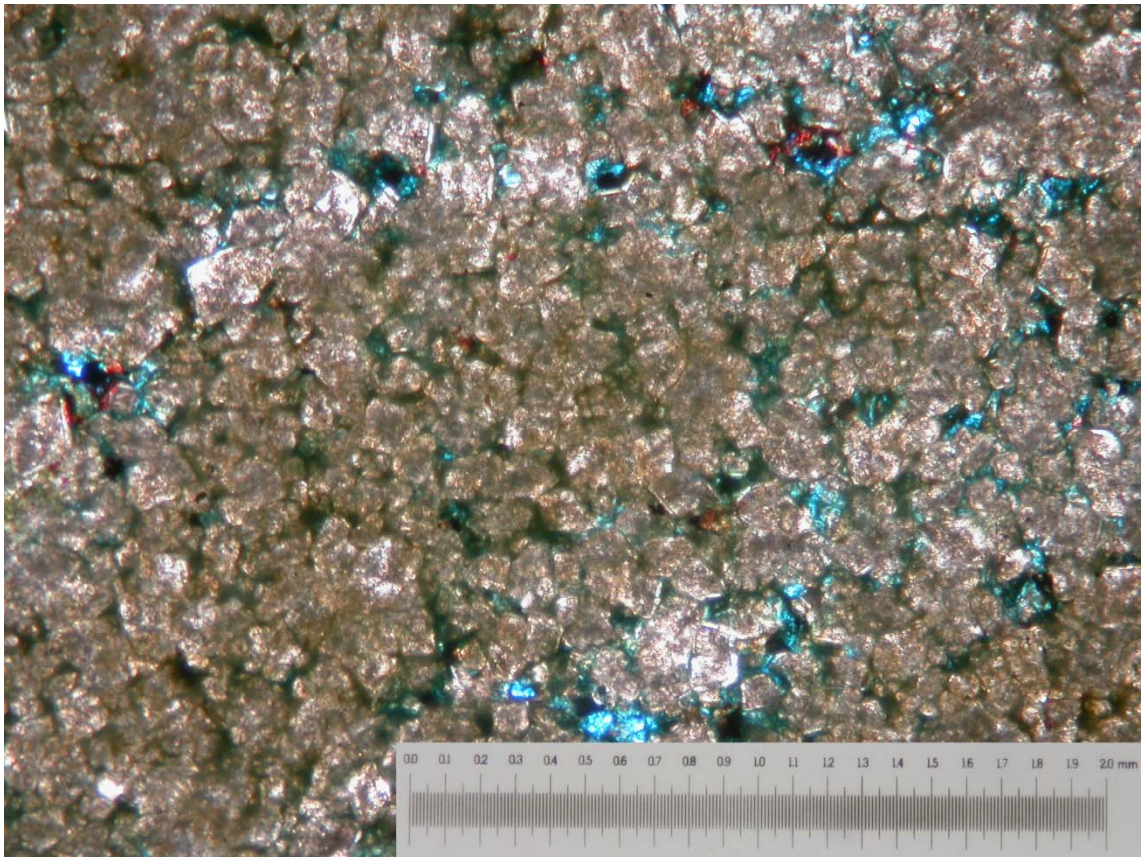

Figure 11. Thin Section – Kasota Dolomite

The Kasota Valley Dolomite appears to have a relatively low porosity and is composed primarily of anthracite and dolomitic crystals, with very little presence of calcite. There appear to be some inter crystalline pores as well as some moldic pores. Grains appear to be highly interlocked.

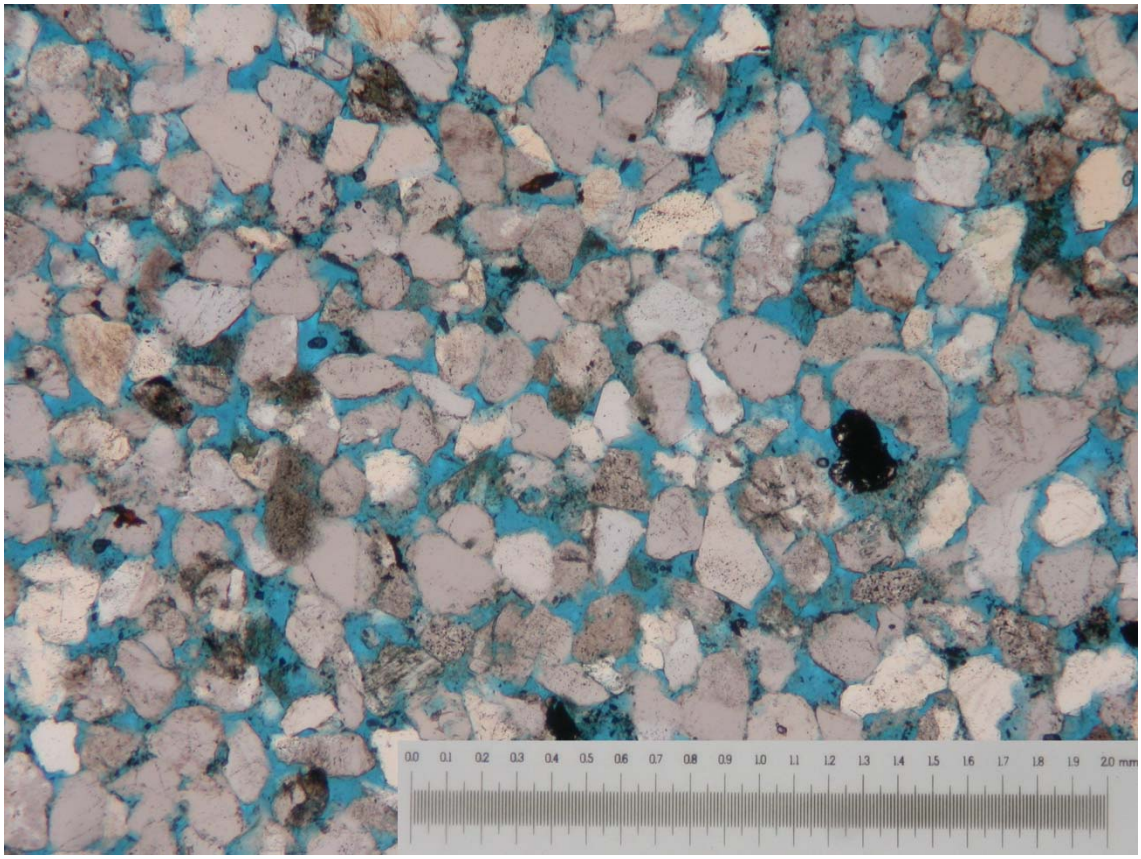

Figure 12. Thin Section – Berea Sandstone

Berea Sandstone is a relatively coarse grained, high porosity rock composed primarily of quartz and its porosity is predominantly inter-crystalline. Grains are highly angular, and there seems to be some interlocking between the quartz grains.

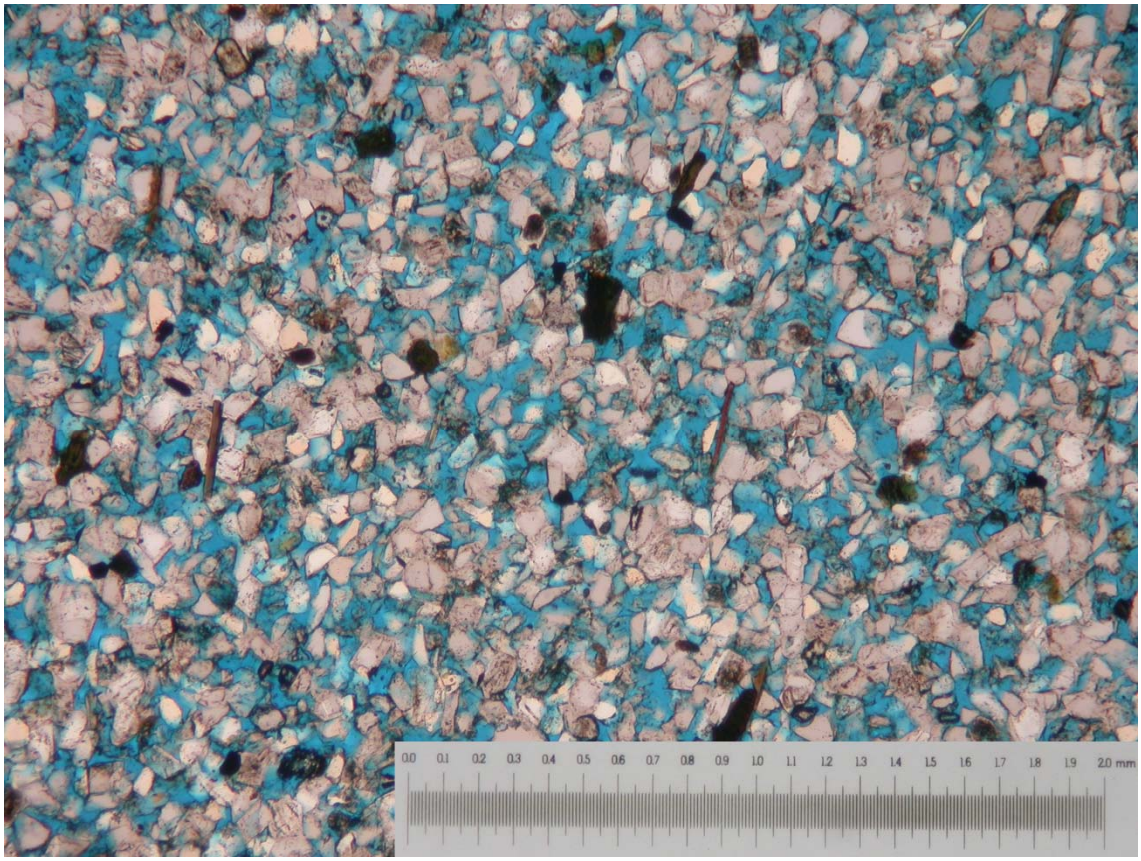

Figure 13. Thin Section – DunnVille Sandstone

DunnVille Sandstone is finer grained than Berea Sandstone, and appears to be more porous. It is composed primarily of quartz and its porosity is predominantly inter-crystalline. Grains are highly angular, and there seems to be some interlocking between the quartz grains.

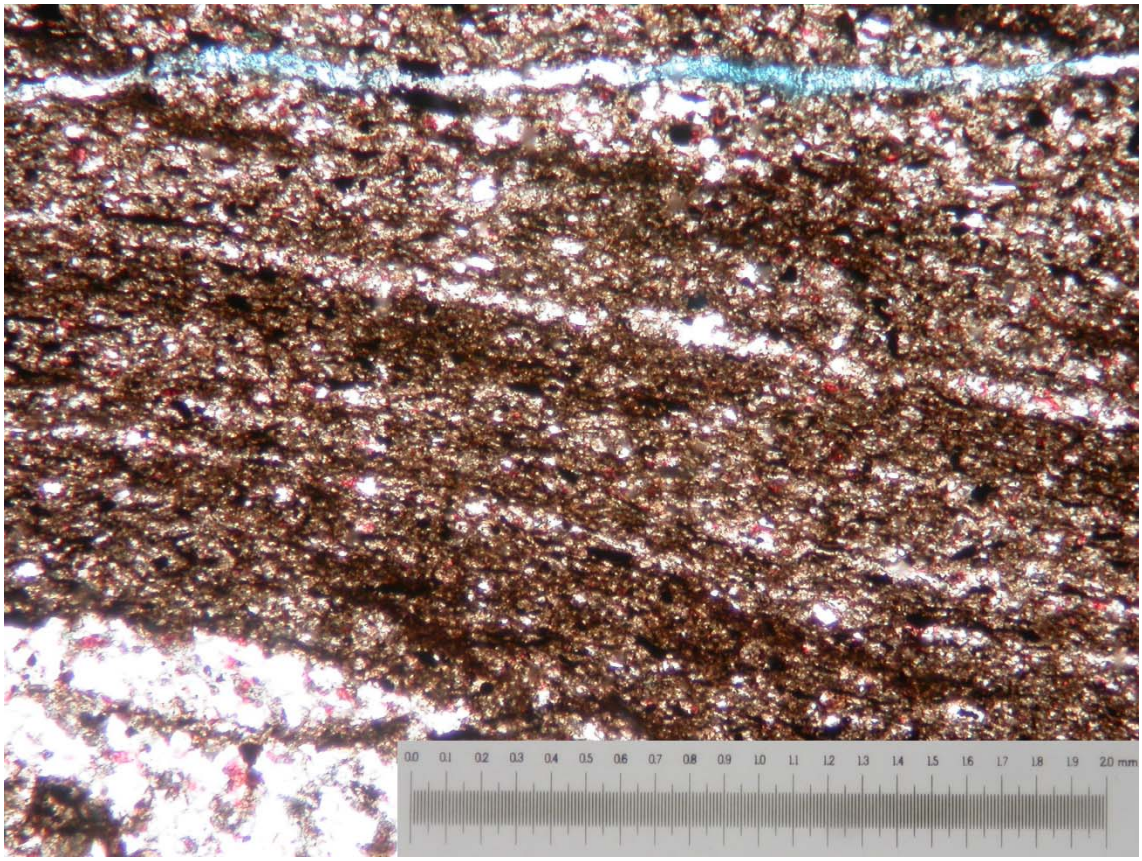

Figure 14. Thin Section – Mancos Shale

Mancos Shale is extremely fine grained, and appears to have significant amount of quartz (white), and calcite (red). Porosity is too small to be observed at these scales, however, the presence of microcracks is evident and is a source of secondary porosity.

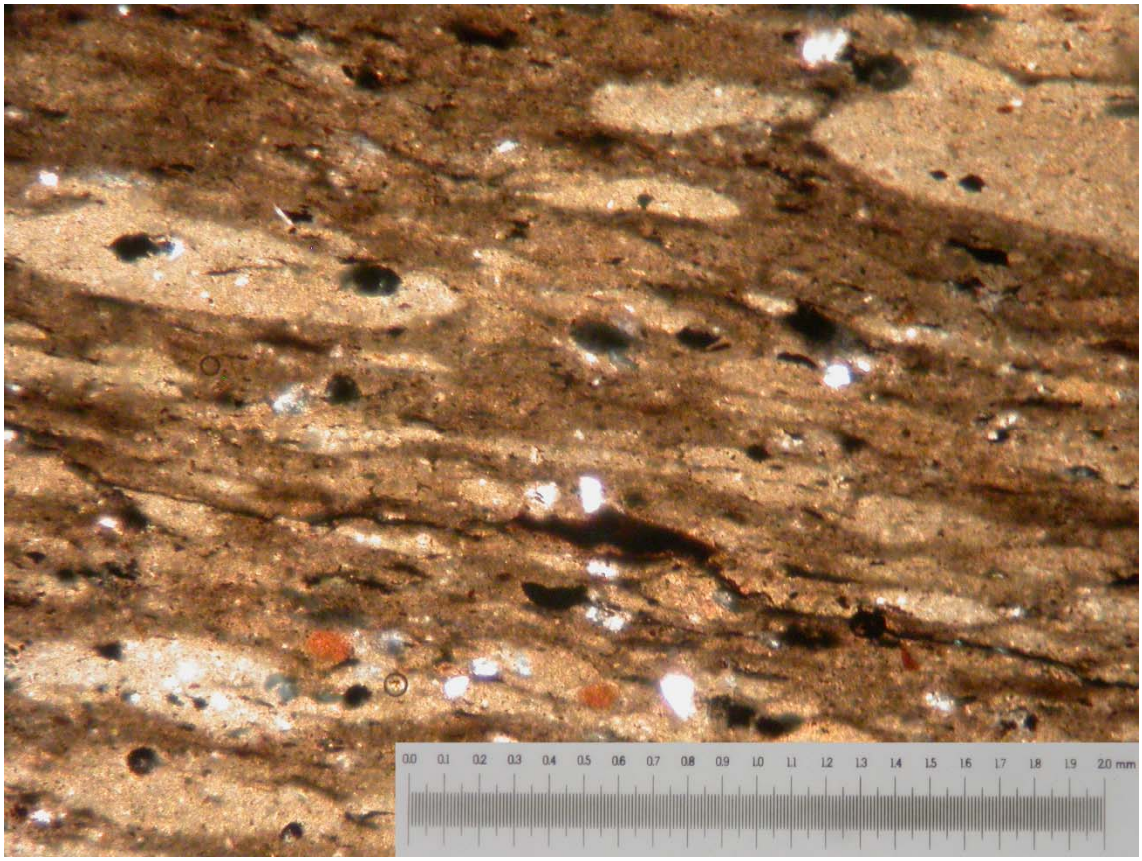

Figure 15. Thin Section – Pierre Shale

Pierre Shale is also extremely fine grained. Porosity is too small to be observed at these scales. The overall grain structure suggests significant quantities of soft sediments that have deformed within the rock matrix. This is corroborated by the high quantities of clay minerals present in this rock type (see mineralogy Appendix A).

Overall, we observe that the index properties of rocks measure herein tend to reflect their pore structures. Softer rocks appear to have higher porosities (Desert Pink Limestone, DunnVille Sandstone), or significant presence of soft sediments (Pierre Shale). Harder rocks are usually not as porous, and have a high degree of interlocking between the grains in the rock matrix (Kasota Dolomite, Berea Sandstone). The

presence of microcracking, indicates the tendency of the rock type to fracture rather than to deform plastically and is another indication of higher hardness values (Mancos Shale).

Chapter 5: Conclusions

A total of twelve different rock types were tested using the Brinell and rebound hardness methods, including four different limestones, four sandstones and four shales. The results show the mechanical rock properties reflect their texture and thus their pore geometry. Softer rocks appear to have higher porosities, or significant presence of soft sediments. Low porosity rocks are usually harder, and have a high degree of interlocking between the grains in the rock matrix. Presence of microcracking is also another indication of higher values for rock hardness. Conventional indentation tests suffer several drawbacks for use over a variety of lithologies in rock mechanics testing. Creep dependency, the limited load range over which they can be performed, and the inability to perform tests on hard rock grades such as metamorphic and igneous rocks (particularly problematic for indexing in geothermal reservoirs) all pose major practical limitations for consistent index testing with the Brinell method. The use of the rebound hammer as an index test overcomes these issues, and since the two indices correlate directly, separately obtained readings from either test may be compared. For these reasons the rebound hammer is proposed to be the better test of the two, and is recommended to be established as the standard for non-destructive index testing in rock mechanics. Further understanding into the relationship between rebound hardness and rock mechanical properties (based on more rigorous theoretical considerations), would be useful in improving the scope and applicability of the rebound hardness test.

References

[1] Van der Vlis, A.C. (1970). Rock Classification by a Simple Hardness Test. In: Proc. 2nd Congress ISRM, pp. 23-30.

[2] Geertsma,J. (1985) Some Rock Mechanical Aspects of Oil and Gas Well Completions. Soc. Petr. Eng. J. 25, 848-856.

[3] Santarelli, F. J., Detienne, J. L., & Zundel, J. P. (1991, January 1). The Use of a Simple Index Test In Petroleum Rock Mechanics. American Rock Mechanics Association.

[4] Zhou, J., Jung, C. M., Chenevert, M. E., & Sharma, M. M. (2013, January 1). Petrophysical Characterization of Organic-Rich Shales: A New Standardized Protocol. American Rock Mechanics Association.

[5] Mueller, M., & Amro, M. (2015, June 3). Indentation Hardness for Improved Proppant Embedment Prediction in Shale Formations. Society of Petroleum Engineers.

[6] Kias, E., Maharidge, R., & Hurt, R. (2015, September 28). Mechanical Versus Mineralogical Brittleness Indices Across Various Shale Plays. Society of Petroleum Engineers.

[7] Rock Properties. (n.d). Retrieved April 06, 2016, from http://www.corelab.com/ps/core-based-strength-logs

[8] Kurz, B. A., Schmidt, D. D., & Cortese, P. E. (2013, February 4). Investigation of Improved Conductivity and Proppant Applications in the Bakken Formation. Society of Petroleum Engineers.

[9] Yasar, S., & Yilmaz, A. O. (2015, January 1). Comparison of Mechanical Strength Prediction with Schmidt Hammer Rebound Value and Rebound Coefficient. International Society for Rock Mechanics.

[10]O. Katz, Z. Reches, J.-C. Roegiers, Evaluation of mechanical rock properties using a Schmidt Hammer, International Journal of Rock Mechanics and Mining Sciences, Volume 37, Issue 4, 1 June 2000, Pages 723-728

[11] McClave, G. A. (2014, August 28). Correlation of Rebound-Hammer Rock Strength With Core and Sonic-Log-Derived Mechanical Rock Properties in Cretaceous Niobrara and Frontier Formation Cores, Piceance Basin, Colorado Society of Petroleum Engineers.

[12] Bagde, M. N., & Chakraborty, A. K. (2009, January 1). Schmidt Hammer As a Rock Mass Characterization Tool. International Society for Rock Mechanics.

[13] Ritz, E., Honarpour, M. M., Dvorkin, J., & Dula, W. F. (2014, August 28). Core Hardness Testing and Data Integration for Unconventionals. Society of Petroleum Engineers.

[14] Lee, J. S., Smallwood, L., & Morgan, E. (2014, August 18). New Application of Rebound Hardness Numbers to Generate Logging of Unconfined Compressive Strength in Laminated Shale Formations. American Rock Mechanics Association.

[15] Haramy, K. Y., & DeMarco, M. J. (1985, January 1). Use Of The Schmidt Hammer For Rock And Coal Testing. American Rock Mechanics Association.

[16] R J Kent (1983) Indentation processes in poly(methylmethacrylate). II. Cone indentation and deep punching J. Phys. D: Appl. Phys. 16 135.

[17] Taylor, P. G. and Appleby, R. R., 2006, Integrating Quantitative and Qualitative Rock Strength Data in Sanding Prediction Studies: An Application of the Schmidt Hammer Method: SPE/IADC Indian Drilling Technology Conference and Exhibition, 101968.

[18] ASTM D5873: American Society for Testing and Materials

[19] Ye, Z. and Ghassemi, A. 2016. Deformation Properties of Saw-Cut Fractures in Barnett, Mancos and Pierre Shales. Accepted by 50th US Rock Mechanics/ Geomechanics Symposium, Houston, Texas, USA, June 26-19 2016.

Appendix A: Mineralogy Reports

Table 3. Mineralogy – Oolitic Limestone

Mineral	Weight %
Calcite	98.5
Quartz	1.5

Table 4. Mineralogy – Indiana Limestone

Mineral	Weight %
Calcite	100

Table 5. Mineralogy –Desert Pink Limestone

Mineral	Weight %
Calcite	99.3
Quartz	0.7

Table 6. Mineralogy –Berea Sandstone

Mineral	Weight %
Quartz	93.5
Illite	3.4
Microcline	2.5
Kaolinte	0.3
Calcite	0.2

Table 7. Mineralogy –Kasota Dolomite

Mineral	Weight %
Ankerite	75.5
Dolomite	17.7
Orthoclase	2.5
Quartz	2.5
Calcite	1.2
Microcline	0.5
Albite	0.3

Table 8. Mineralogy –Scioto Sandstone

Mineral	Weight %
Quartz	71.5
Muscovite	8.8
Orthoclase	8.2
Albite	8.3
Chlorite	2
Kaolinte	1.3

Table 9. Mineralogy –Dunnville Sandstone

Mineral	Weight %
Quartz	46.6
Microcline	34
Sanidine	12.6
Orthoclase	6.3
Muscovite	0.5

Table 10.Mineralogy –JackFork Sandstone

Mineral	Weight %
Quartz	76.8
Muscovite	9.1
Illite	3.5
Sanidine	2.8
Clinochore	3.1
Kaolinite	2.4
Siderite	2.4

Table 11.Mineralogy –Pierre Shale

Mineral	Weight %
Quartz	36.5
Muscovite	15.9
Albite	13.3
Kaolinite	11.5
Orthoclase	6.7
Calcite	7.2
Chlorite	5.4
Sanidine	2.1
Pyrite	2.3

Table 12.Mineralogy –Barnett Shale

Mineral	Weight %
Muscovite	34.6
Quartz	28.7
Illite	23.2
Kaolinite	5.1
Microcline	4.9
Pyrite	2.7
Chlinochlore	0.7

Table 13.Mineralogy –Mancos Shale

Mineral	Weight %
Quartz	49.9
Muscovite	18.8
Dolomite	10.8
Calcite	7.8
Sanidine	4.6
Kaolinite	4.3
Albite	3.2
Pyrite	0.6

Table 14.Mineralogy –Green River Shale

Mineral	Weight %
Calcite	28.8
Analcime	21.2
Albite	16.6
Quartz	15.6
Sodium Aluminum Silicate	6.5
Illite	6.1
Siderite	5.2

Appendix B: Tabulated Test Data

Table 15. Brinell Hardness Test Data

Rock	Force (kgF)	Ball Size (mm)	Indent Size (mm)	BHN	Average BHN	Standard Deviation
Oolitic Limestone	25.49	3.00	1.31	17.96	18.41	0.635957309
	25.49	3.00	1.28	18.86		
Indiana Limestone	25.49	3.00	0.92	37.43	36.23	1.686705697
	25.49	3.00	0.95	35.04		
Desert Pink Limestone	25.49	3.00	1.38	16.09	13.90	3.101805561
	25.49	3.00	1.60	11.70		
Kasota Dolomite	25.49	3.00	0.58	95.58	90.95	6.546546912
	25.49	3.00	0.61	86.32		
Berea Sandstone	25.49	3.00	0.82	47.35	49.22	2.642608155
	25.49	3.00	0.79	51.09		
Scioto Sandstone	25.49	3.00	0.55	106.39	104.49	2.685780552
	25.49	3.00	0.56	102.59		
Dunnville Sandstone	25.49	3.00	1.15	23.61	22.79	1.149054506
	25.49	3.00	1.19	21.98		
JackFork Channel Fill Sandstone	25.49	3.00	0.62	83.53	87.93	6.227045289
	25.49	3.00	0.59	92.33		
Mancos Shale	25.49	3.00	0.48	139.97	131.93	11.37549574
	25.49	3.00	0.51	123.88		
Pierre Shale	25.49	3.00	1.60	11.70	12.30	0.84444115
	25.49	3.00	1.53	12.90		
Barnett Shale	25.49	3.00	1.09	26.39	25.00	1.965971695
	25.49	3.00	1.15	23.61		
Green River Shale	25.49	3.00	0.39	212.50	202.34	14.36308878
	25.49	3.00	0.41	192.19		

Average Standard Deviation (Brinell Hardness): 4.43

Table 16. Rebound Hardness Data – Carbonates

	Oolitic Limestone	Indiana Limestone	Desert Pink Limestone	Kasota Dolomite
	381	405	300	541
	396	415	332	463
	430	398	324	606
	406	393	309	405
	397	411	349	499
	401	400	327	531
	394	427	331	489
	417	446	308	557
	389	409	338	528
	401	487	332	525
Mean	401.2	419.1	325	514.4
Standard Deviation	13.97	28.42	15.11	54.75

Table 17. Rebound Hardness Data – Sandstones

	Berea Sandstone	Scioto Sandstone	Dunville Sandstone	JackFork Upper Sandstone
	554	507	447	550
	499	531	409	584
	516	505	445	620
	484	542	443	539
	497	533	413	407
	468	549	434	419
	474	547	432	627
	523	558	451	610
	562	555	454	536
	523	534	424	489
Mean	510	536.1	435.2	538.1
Standard Deviation	31.69	18.29	15.69	78.75

Table 18. Rebound Hardness Data – Shale

	Mancos Shale	Pierre Shale	Barnett Shale	Green River Shale
	555	367	439	598
	574	371	449	684
	609	377	443	654
	620	264	437	666
	634	368	459	630
	612	222	433	692
	575	335	449	655
	588	336	458	713
	578	307	472	653
	621	296	454	622
Mean	596.6	324.3	449.3	656.7
Standard Deviation	25.95	51.79	11.88	34.37

Average Standard Deviation (Rebound Hardness): 31.72